Journal of Applied Mechanics and Technical Physics, Vol. 50, No. 1, pp. 35–43, 2009

PHYSICOMATHEMATICAL MODELING OF THE PROCESSES OF CAPILLARY IMPREGNATION OF POROUS MATERIALS

A. A. Zhilin and A. V. Fedorov

UDC 539.219

The process of capillary impregnation of porous materials is studied numerically. A physicomathematical model of liquid diffusion in a porous sample is proposed. The model involves an analytical presentation of the diffusion coefficient, which describes available experimental data. A method of solving one-dimensional unsteady problems of impregnation is developed and tested on a self-similar solution of the corresponding boundary-value problem of impregnation. If the impregnation process is sufficiently long, the motion of the liquid in the sample is described by a stable self-similar solution. A classification of moisture diffusion on the basis of the initial humidity on the sample boundary is proposed.

Key words: *capillary impregnation, porous materials, diffusion.*

Introduction. The use of porous materials of the new generation in civil engineering and some other branches of industry makes it necessary to study the specific features of the mechanism of moisture interaction with porous materials. These issues were studied in numerous papers (see, e.g., [1–3]). In particular, Nizovtsev et al. [1] described experimental data on moisture penetration into a porous material and, based on their experiments, determined the dependence of the diffusion coefficient of moisture on its concentration in the porous material.

The present paper reports the results of mathematical modeling of the process of moisture migration in a porous skeleton of a solid material. The main goal is to study the flow pattern formed owing to the contact between the porous skeleton and the water surface and to determine the effect of the initial parameters of the liquid–solid system on the character of liquid diffusion.

Physicomathematical Formulation of the Problem. Let us consider a vertically aligned beam made of a porous material (autoclave-cured aerated concrete) whose side walls are permeable for moisture, and the lower surface contacts the water surface. The upper plane is a free surface and has a constant humidity. The beginning of the impregnation process is the moment of the contact between the dry face of the beam and the humid medium ($t = 0$). After the contact, a humidity wave propagates in the porous material. The task is to determine the flow pattern of the liquid in the porous beam at subsequent times ($t > 0$).

To describe the examined process, we use the equation of unsteady diffusion in the form

$$\frac{\partial W}{\partial t} = \frac{\partial}{\partial x}\Big(D(W)\,\frac{\partial W}{\partial x}\Big), \tag{1}$$

where $D(W)$ is the diffusion coefficient, W is the humidity, t is the time, and x is the spatial coordinate.

Equation (1) is supplemented by the initial conditions

$$t = 0: \qquad W = \begin{cases} W_0, & x = 0, \\ 0, & 0 < x \leqslant l \end{cases} \tag{2}$$

and by the boundary conditions

Khristianovich Institute of Theoretical and Applied Mechanics, Siberian Division, Russian Academy of Sciences, Novosibirsk 630090; lab20@itam.nsc.ru. Translated from Prikladnaya Mekhanika i Tekhnicheskaya Fizika, Vol. 50, No. 1, pp. 42–51, January–February, 2009. Original article submitted July 19, 2007; revision submitted October 4, 2007.

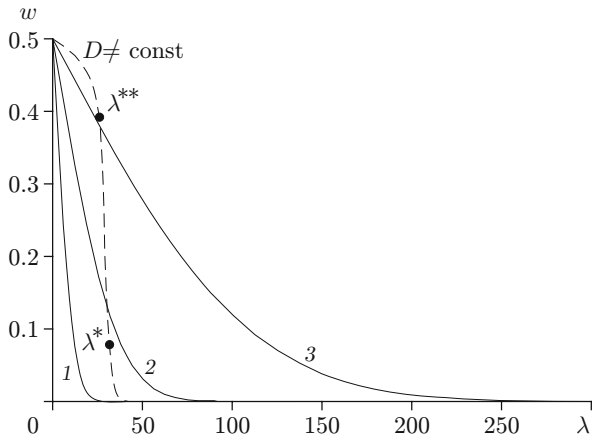

Fig. 1

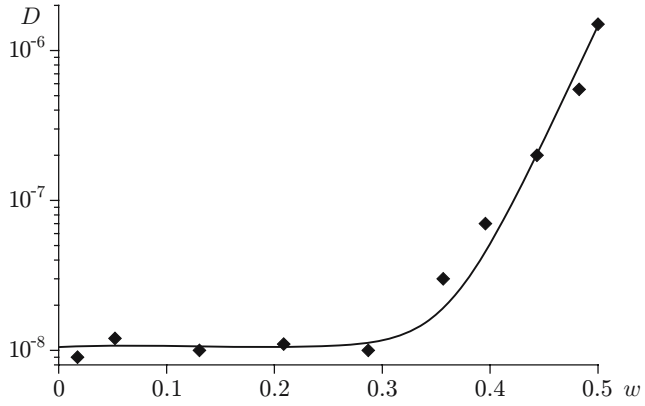

Fig. 2

Fig. 1. Permeability versus the diffusion coefficient: $D = 10^{-8}$ (1), 10^{-7} (2), and 10^{-6} m^2/sec (3).

Fig. 2. Interpolation of experimental data (points) by the exponential function (7) (solid curve).

$$x = 0: \quad W = W_0, \qquad x = l: \quad \frac{\partial W}{\partial x} = 0. \tag{3}$$

Self-Similar Approximation. Let us pass to new variables t and $\lambda = x/\sqrt{t}$, in which Eq. (1) acquires the following form:

$$t\,\frac{\partial w}{\partial t} = \frac{\lambda}{2}\,\frac{\partial w}{\partial \lambda} + \frac{\partial}{\partial \lambda}\Big(D(w)\,\frac{\partial w}{\partial \lambda}\Big). \tag{4}$$

Problem (2)–(4) was solved numerically by the shooting method in two steps.

Step 1. Let us assume that the diffusion coefficient is constant: $D(w) = \text{const} = D$. Then the diffusion equation in the self-similar variables (4) can be written in the form

$$t\,\frac{\partial w}{\partial t} = \frac{\lambda}{2}\,\frac{\partial w}{\partial \lambda} + D\,\frac{\partial^2 w}{\partial \lambda^2}. \tag{5}$$

In the steady approximation, Eq. (5) with the boundary conditions (3) can be presented in the form

$$w'' = -\lambda w'/(2D); \tag{6}$$

$$\lambda = 0: \quad w = w_0, \qquad \lambda = +\infty: \quad w = 0.$$

The solution of Eq. (6) has the form

$$w = w_0[1 - \text{Erf}\,(\lambda/(2\sqrt{D}\,))].$$

Below we compare the liquid flows in a porous body characterized by the minimum and maximum values of the diffusion coefficient and by the variable quantity $D = D(w)$. Let us consider the behavior of the solution obtained as a function of the diffusion coefficient D. Figure 1 shows the solutions of Eq. (6) for the values of the diffusion coefficient $D = 10^{-6}$, 10^{-7}, and 10^{-8} m^2/sec. Naturally, the magnitude of permeability decreases with decreasing diffusion coefficient; hence, curve 2 in Fig. 1 lies higher than curve 1 corresponding to a smaller value of the permeability coefficient.

To test the method of solving the boundary-value problem for a self-similar flow with $D = \text{const}$, we solved Eq. (6) numerically by the shooting method. The boundary conditions on the left boundary were prescribed values of the function $w(0) = w_0$ and its first derivative $w'(0) = w'_0$. The value of w_0 in all cases was 0.5, and the value of w'_0 was chosen to satisfy the condition $|w(\lambda_i)| < \varepsilon$, where λ_i is the final size of the computational domain. The values used were $w'_0 = -0.00470$ for $D = 10^{-6}$ m^2/sec, $w'_0 = -0.014\,86$ for $D = 10^{-7}$, and $w'_0 = -0.04703$ for $D = 10^{-8}$. It turned out that the numerical solution coincides with the analytical solution.

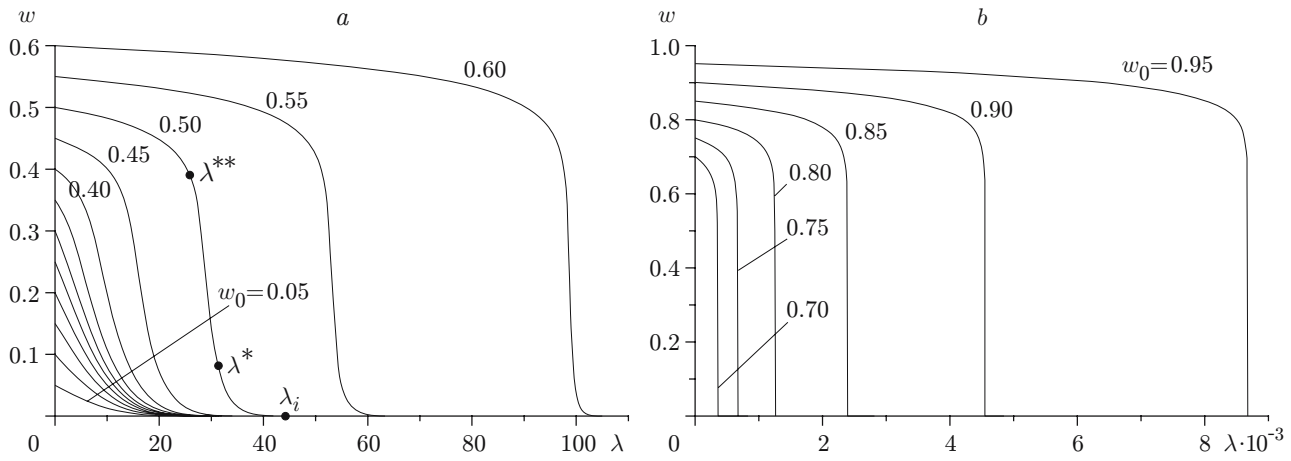

Fig. 3. Permeability versus the initial humidity: $w_0 < 0.6$ (a) and $w_0 > 0.7$ (b).

TABLE 1

Parameters of the Humidity Wave in the Self-Similar Approximation

w_0	λ_i	$\lambda_{\max}$	$w'_{\max}$	$w_{\max}$	$l_{\Pr}$
0.05	26.9	0.1	0.00459	0.04954	10.8994
0.10	28.7	0.1	0.00915	0.09908	10.9244
0.15	29.7	0.2	0.01365	0.14727	10.9851
0.20	30.3	0.9	0.01796	0.18391	11.1568
0.25	30.9	2.0	0.02176	0.20740	11.4887
0.30	31.4	3.4	0.02551	0.22149	11.7604
0.35	32.1	5.4	0.03025	0.23091	11.5707
0.40	33.4	8.9	0.03855	0.23999	10.3759
0.45	36.5	15.7	0.05527	0.24645	8.1417
0.50	44.2	28.6	0.08925	0.25149	5.6021
0.55	63.0	52.9	0.15631	0.25206	3.5187
0.60	104.5	98.5	0.22680	0.28865	2.6455
0.65	188.0	185.0	0.33578	0.31858	1.9358
0.70	350.0	348.8	0.58762	0.08184	1.1913
0.75	651.3	651.0	0.92828	0.60630	0.8079

In solving the boundary-value problem for Eq. (5) numerically, we used the method of lines. The resultant system of ordinary differential equations was solved by a method based on the formula of backward differentiation. For sufficiently long durations of the impregnation process, the numerical solution obtained by the method of lines for three values of the diffusion coefficient also coincides with the previously found analytical and numerical solutions of the steady-state equation (6).

Step 2. Let us find the solution of the initial-boundary problem for the original equation (4) with a variable value of the diffusion coefficient. The dependence of the diffusion coefficient on humidity was found by interpolating the experimental data [1]. It is seen from Fig. 2 that the experimental data are adequately described by an exponential expression in the form

$$D(w) = a_0 + c_0 \exp\left((w - w_p)/c\right), \tag{7}$$

where $a_0 = 1.05 \cdot 10^{-8}$, $c_0 = 3 \cdot 10^{-8}$, $w_p = 0.36$, and $c = 0.037$.

In the steady-state approximation, Eq. (4) was solved by the shooting method. The solutions of this equation for different values of w_0 are plotted in Fig. 3a. The resultant solution is the humidity profile in self-similar variables, where three segments can be identified. The first segment is characterized by the increase in humidity from the value $w_0 = 0$ at $\lambda = +\infty$ to the value $w_0 = w^*$ at $\lambda = \lambda^*$. We replace the point $\lambda = +\infty$ by the point $\lambda = \lambda_i$, where the humidity differs from zero by a small quantity $\varepsilon = 10^{-4}$. The values of λ_i for different values of the initial humidity are listed in Table 1. Thus, the total width of the humidity profile in the self-similar variables is $\lambda_i = 44.2$.

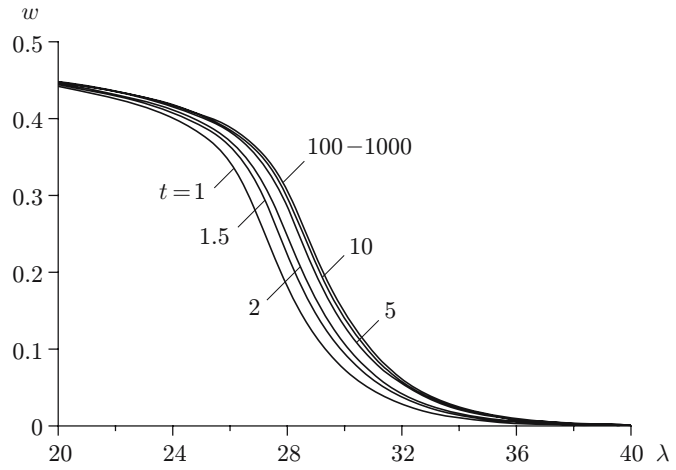

Fig. 4. Steady-state profile of humidity obtained by a time-dependent method in the self-similar approximation.

The second segment is located between the points $\lambda = \lambda^*$ and $\lambda = \lambda^{**}$ (see Figs. 1 and 3a). The length of this segment is determined by the wave width according to Prandtl ($l_{\mathrm{Pr}} = 5.6021$). The segment under consideration, which is characterized by a drastic increase in humidity, contains an inflection point behind which the humidity profile is no longer concave, but becomes convex. In addition, this segment contains the point $\lambda = \lambda_{\max}$ with the maximum gradient of humidity. This point corresponds to the maximum values of humidity $w_{\max}$ and its derivative $w'_{\max}$. For the initial humidity $w_0 = 0.5$, these values are $\lambda_{\max} = 28.6$, $w_{\max} = 0.25149$, and $w'_{\max} = 0.08925$ (see Table 1). The third segment of the humidity profile begins at the point $\lambda = \lambda^{**} \approx 25.8$ and ends at the point $\lambda = 0$. The humidity profile on this segment has a convex shape.

The initial-boundary problem (2)–(4) was solved in an unsteady approximation by a time-dependent method. Figure 4 shows the humidity profiles obtained at the times $t = 1$, 1.5, 2, 5, 10, and 100. Note that the humidity profile at $t = 100$ coincides with the profiles obtained previously in the steady-state approximation. The humidity profile remains unchanged after $t > 1000$, i.e., it is identical to that at $t = 100$ (see Fig. 4). Thus, as $t \to \infty$, we obtain a steady-state self-similar liquid flow in a porous sample.

Effect of the Initial Humidity. Let us consider the effect of the initial humidity on the flow in the sample. Figure 3 shows the distributions of the humidity w as a function of the self-similar variable λ with the initial humidity w_0 being changed from 0.05 to 0.95 with a step of 0.05. For small values $w_0 \leqslant 0.15$, the humidity profile is concave. The maximum gradient of humidity $w'_{\max}$ is on the left boundary; hence, there are no second and third segments (see Fig. 3a). Therefore, there is no wave front of impregnation for these parameters. As the initial humidity is increased from $w_0 = 0.15$ to $w_0 = 0.35$, the maximum gradient of humidity is shifted from the left boundary toward higher values of λ (see Table 1), and the second segment appears. Beginning from the value $w_0 = 0.35$, there appears the third segment. With a further increase in the initial humidity, the maximum value of the humidity gradient $\lambda_{\max}$ is shifted toward higher values of λ (see Table 1), which is caused by intense growth of the diffusion coefficient as a function of humidity (see Fig. 2).

The following specific features are observed as w_0 is increased from $w_0 = 0.5$ to $w_0 = 0.95$: 1) the size of the precursor region gradually decreases and reaches the size of the step over the self-similar variable at $w_0 = 0.75$; later this region disappears (see Fig. 3); 2) the wave width according to Prandtl gradually decreases, and there arises an "internal discontinuity" at $w_0 = 0.7$ ($\lambda_{\max} = 348.8$ and $w_{\max} = 0.08184$). At $w_0 \geqslant 0.75$, the amplitude of the "discontinuity" increases and the length of the second segment, i.e., the wave width, decreases ($l_{\mathrm{Pr}} \to 0$). Finally, the length of the third segment increases substantially (almost by a factor of 2 at each step $\Delta w_0 = 0.05$). This means that the wave mechanism of impregnation is in operation, which involves a drastic increase in saturation in a certain region of moderate length. After that, humidity relaxation to the boundary value is observed.

TABLE 2

Dynamics Parameters of Humidity Waves in the Plane of Physical Variables

t	x_i	$x_{\max}$	$W'_{\max}$	$W_{\max}$	$l_{\Pr}$
			$W_0 = 0.3$		
1	40.7	3.2	0.02691	0.22193	11.150
2	59.8	4.7	0.01851	0.22108	16.212
5	96.1	7.5	0.01152	0.22183	26.053
10	136.6	11.0	0.00811	0.21908	37.014
20	192.0	15.4	0.00573	0.21987	52.402
50	305.2	24.4	0.00362	0.21990	82.988
100	433.0	37.1	0.00255	0.21372	117.647
200	610.1	52.9	0.00181	0.21260	166.205
500	954.6	81.3	0.00115	0.21519	262.009
1000	1370.8	116.3	0.00081	0.21440	370.370
			$W_0 = 0.5$		
1	49.6	27.1	0.09371	0.25312	5.336
2	72.4	39.4	0.06439	0.25113	7.765
5	116.2	63.2	0.04032	0.25096	12.402
10	164.9	90.0	0.02836	0.25059	17.634
20	234.3	127.5	0.02001	0.25232	24.988
50	370.7	202.1	0.01265	0.25000	39.526
100	525.4	285.5	0.00891	0.25339	56.148
200	742.9	404.2	0.00630	0.25151	79.428
500	1172.5	639.1	0.00400	0.25226	125.156
1000	1657.1	904.0	0.00281	0.25062	177.936
			$W_0 = 0.7$		
1	333.8	331.1	0.90848	0.20379	0.771
2	485.2	481.3	0.66855	0.22144	1.047
5	779.3	773.1	0.44316	0.24296	1.580
10	1107.9	1099.0	0.31467	0.24130	2.225
20	1570.8	1558.1	0.22295	0.26611	3.140
50	2488.3	2467.4	0.13681	0.25965	5.117
100	3520.8	3491.3	0.09675	0.25106	7.236
200	4980.5	4938.6	0.06865	0.25796	10.197
500	7876.0	7809.9	0.04335	0.25378	16.150
1000	11,133.5	11,039.9	0.03068	0.25411	22.812

Solution in the Domain of Physical Variables. Let us now pass to solving the problem posed in the plane of physical variables x and t. The initial-boundary problem (1)–(3) was solved numerically by the method tested above.

Propagation of the Humidity Wave. Figure 5 shows the humidity profiles at the times $t = 1$–10 with the step equal to 1, $t = 10$–100 with the step equal to 10, and $t = 100$–1000 with the step equal to 100 for the initial values of humidity $W_0 = 0.3$ (Fig. 5a), 0.5 (Fig. 5b), and 0.7 (Fig. 5c). The values of the main parameters of the humidity profiles are summarized in Table 2. Analyzing the humidity profiles for $W_0 = 0.3$, we see that the size of the region of filtration impregnation increases intensely with time, i.e., $x_i \gg x_{\max}$. With increasing t, the humidity profile becomes less steep, the maximum value of the humidity gradient decreases ($W'_{\max} \to 0$), and, as a consequence, the width of the humidity profile according to Prandtl increases.

At $W_0 = 0.5$, the character of humidity wave propagation becomes substantially different. In particular, the velocity of propagation of the filtration precursor remains almost the same as that at $W_0 = 0.3$, while the velocity of the inflection point on the profile (wave center) increases and reaches approximately 50% of the precursor velocity. Moreover, at $W_0 = 0.5$, the width of the humidity profile according to Prandtl decreases almost twofold, as compared with the case with $W_0 = 0.3$ (see Table 2).

An increase in the initial humidity to $W_0 = 0.7$ changes the shape of the humidity profile. The profile contains a small filtration segment, a segment with a jumplike increase in humidity, and a segment where the value of humidity increases to its boundary value. As moisture propagates over the porous material, the slope of the

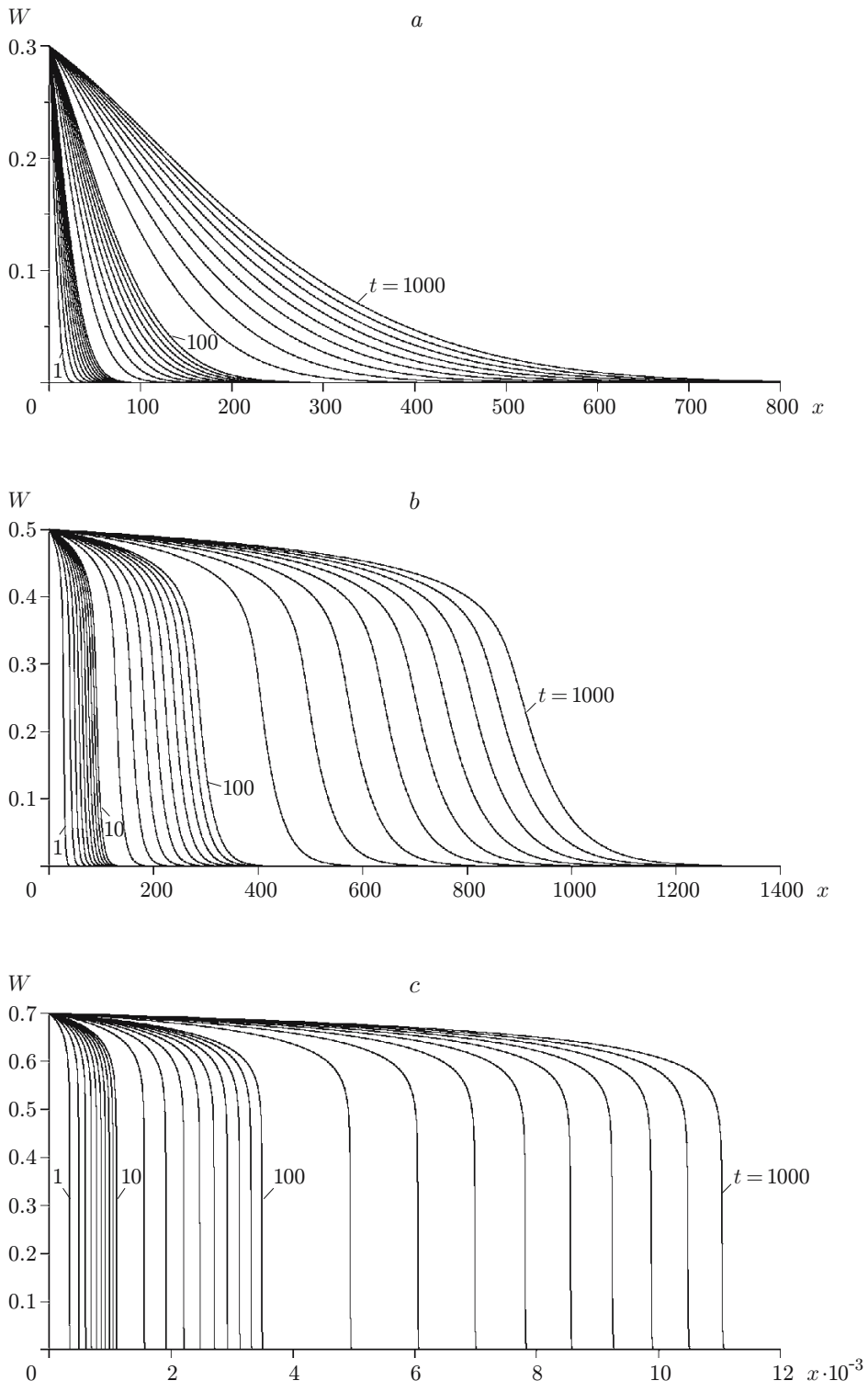

Fig. 5. Propagation of the humidity wave: $W_0 = 0.3$ (a), 0.5 (b), and 0.7 (c).

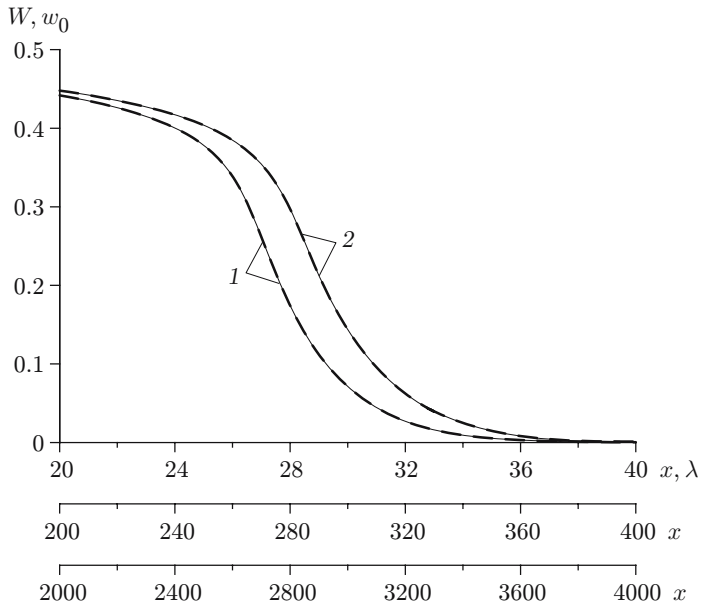

Fig. 6. Results calculated in the plane of physical variables (solid curves) and self-similar variables (dashed curves): 1) $t = 1$ and $l = 100$; 2) $t = 100$–$10{,}000$ and $l = 1000$–$10{,}000$.

humidity profile increases, but the width of the humidity profile according to Prandtl is almost eight times smaller than that at $W_0 = 0.5$ and 16 times smaller than that at $W_0 = 0.3$. Note that the velocity of the humidity wave increases substantially (almost by a factor of 10), as compared with the case of $W_0 = 0.5$. It follows from Fig. 5c that the most significant change in the shape of the humidity profile occurs on the third segment whose length rapidly increases and approaches the width of the humidity profile. Note, the velocity of propagation of the humidity profile decreases with time, in particular, it decreases by a factor of 10 in the interval $t = 10$–1000. A similar situation is observed at $W_0 = 0.5$ and 0.3. Another specific feature of the humidity profile behavior is the location of the point where the humidity gradient reaches its maximum value (inflection point over the profile height): $W_{\max} \approx 0.22$ (which is 73% of W_0) for $W_0 = 0.3$, $W_{\max} \approx 0.25$ (50%) for $W_0 = 0.5$, and $W_{\max} \approx 0.25$ (35%) for $W_0 = 0.7$. Thus, the inflection point moves over the profile from top down to the value $W_{\max} \approx 0.26$ (approximately 30% of the total height of the profile at $W_0 = 0.9$).

Figure 6 shows the results calculated for $W_0 = 0.5$. The solid curves show the humidity profiles obtained by solving problem (1)–(3) in the physical domain of motion at $t = 1$ and $t = 100$–$10{,}000$ with the length of the computational domain $l = 100$ and $l = 1000$–$10{,}000$, respectively. The scale in this plot is changed unusually: as the length of the domain is increased from $l = 100$ to $l = 1000$ and then to $l = 10{,}000$, the scale on the axis is increased by an order of magnitude. The dashed curves show the results calculated by solving the initial-boundary problem (2)–(4) in the self-similar variables at $t = 1$ and $t = 100$–1000. It should be noted that $l/\sqrt{t} = 100$ in all three cases. It follows from Fig. 6 that the solution obtained in the plane of physical variables coincides with the solution obtained in the self-similar approximation.

Distribution of Humidity over the Cross Sections of the Porous Material. Let us study the dynamics of humidity variation in the cross sections $x = 10, 20, \ldots, 90$ mm in a beam of length $l = 100$ mm, made of a porous material. Figure 7 shows the time evolution of the humidity distributions in the cross sections considered. The humidity profile in each cross section has three segments. The beginning of the first segment with a zero value of humidity corresponds to the beginning of the experiment; the end of this segment corresponds to the moment when the humidity wave reaches the section considered. On the second segment, the humidity gradually increases to W_{fin}. The third segment, like the first one, is characterized by a constant value of humidity equal to W_{fin}. The final values of humidity in the cross sections for different initial values of humidity are given in Table 3. The length of the first segment increases as the cross section considered moves away from the plane of contact with water inward the beam. At $W_0 = 0.1$, the second segment (from $W = W_0$ to $W = W_{\text{fin}}$) reaches the greatest length, which amounts

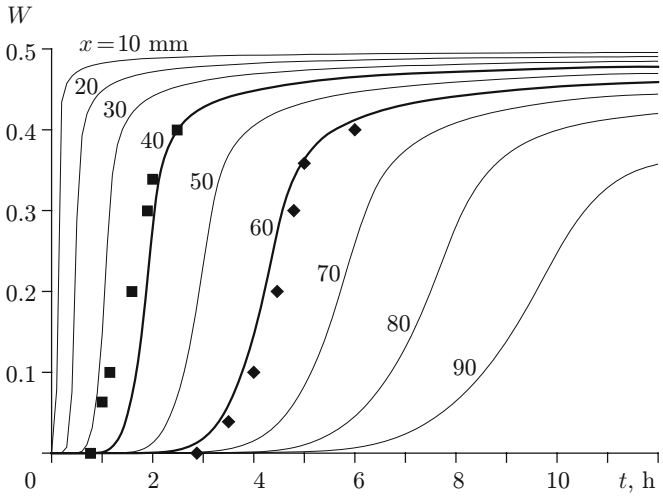

Fig. 7. Cross-sectional distributions of humidity: the curves and points refer to the calculated data and experimental data [1], respectively.

TABLE 3

Limiting Values of Humidity

x, mm	W_{fin}								
	$W_0 = 0.1$	$W_0 = 0.2$	$W_0 = 0.3$	$W_0 = 0.4$	$W_0 = 0.5$	$W_0 = 0.6$	$W_0 = 0.7$	$W_0 = 0.8$	$W_0 = 0.9$
10	0.09011	0.18063	0.27769	0.39176	0.49574	0.59611	0.69644	0.79856	0.89955
20	0.08012	0.16084	0.25141	0.38142	0.49088	0.59172	0.69245	0.79705	0.89909
30	0.07013	0.14090	0.22238	0.36792	0.48529	0.58673	0.68798	0.79547	0.89862
40	0.06013	0.12088	0.19174	0.34905	0.47872	0.58097	0.68290	0.79383	0.89815
50	0.05013	0.10081	0.16029	0.32034	0.47075	0.57414	0.67701	0.79210	0.89767
60	0.04013	0.08071	0.12848	0.27480	0.46063	0.56576	0.66999	0.79029	0.89718
70	0.03012	0.06059	0.09651	0.21226	0.44678	0.55491	0.66133	0.78839	0.89669
80	0.02011	0.04047	0.06447	0.14274	0.42486	0.53952	0.65001	0.78639	0.89620
90	0.01011	0.02034	0.03240	0.07184	0.37239	0.51273	0.63360	0.78427	0.89569

approximately to 1000 h. The value of W_{fin} in different cross sections varies considerably (the maximum change in W_{fin} is 80%).

Verification of the Mathematical Model. Results of numerical calculations obtained by the proposed mathematical model are compared with experimental data [1]. It follows from Fig. 7 that the proposed mathematical model provides an adequate description of experimental data in cross sections $x = 40$ and 60 mm.

Conclusions. A diffusion physicomathematical model of capillary impregnation of a porous material is proposed and verified. The model is based on an analytical expression for the diffusion coefficient, which ensures an adequate description of experimental data.

A method of solving one-dimensional unsteady problems of impregnation is developed and tested on a self-similar solution of the corresponding boundary-value problem of impregnation.

It is found that the liquid flow in the sample is described by a self-similar solution if the impregnation process is sufficiently long. Stability of this solution is demonstrated.

A classification of moisture diffusion depending on the initial humidity on the sample boundary is proposed: 1) smooth impregnation wave; 2) diffusion impregnation wave accompanied by a precursor and a diffusion zone of relaxation to the boundary value of saturation, and 3) wave with a sudden change in its profile.

This work was supported by the Russian Foundation for Basic Research (Grant No. 07-08-00065), President of the Russian Federation on the Support of Young Russian Scientists and Leading Scientific Schools (Grant No. MK-2209.2007.8), and by the Youth Project No. 25 of the Siberian Division of the Russian Academy of Sciences.

REFERENCES

1. M. I. Nizovtsev, S. V. Stankus, A. N. Sterlyagov, et al., "Experimental determination of diffusion coefficients of moisture in porous materials in the case of capillary and sorption humification," *Inzh.-Fiz. Zh.*, **78**, No. 1, 67–73 (2005).
2. A. G. Perekhozhentsev, *Theoretical and Computational Issues of the Humidity State of Inhomogeneous Segments of Building Fences* [in Russian], Volgograd State Academy of Architecture and Civil Engineering, Volgograd (1997).
3. *Development of Research in the Field of the Filtration Theory in the USSR* (*1917–1967*) [in Russian], Nauka, Moscow (1969), Chapter 5.